ELSEVIER

Journal of Alloys and Compounds 244 (1996) 197–205

Journal of ALLOYS AND COMPOUNDS

Site related nucleation and growth of hydrides on uranium surfaces

R. Arkush[a,b], A. Venkert[a], M. Aizenshtein[a], S. Zalkind[a,b], D. Moreno[a], M. Brill[a,b], M.H. Mintz[a,b,*], N. Shamir[a]

[a] *Nuclear Research Center - Negev, PO Box 9001, Beer-Sheva 84190, Israel*
[b] *Ben-Gurion University of the Negev, PO Box 653, Beer-Sheva 84105, Israel*

Received 2 July 1996

Abstract

The characteristics of hydride nucleation and growth on certain surfaces of pure uranium and of U–0.1 wt.% Cr samples were studied (under 1 atm H, at temperatures of 50–75 °C) using the hot-stage microscope, microprobe analyzer and atomic force microscope techniques. Different preparation procedures of the samples were applied, in order to check the effects of surface oxidation layer variations on the nucleation and growth characteristics. Four families of hydride nuclei, differing in density, size and growth rates, were observed and classified. The smallest and most dense is in the form of submicron blisters formed instantaneously along mechanical polishing scratches. A larger (1–10 μm) blister-like family is formed beneath the oxide at point defect sites (but not discontinuities of the oxide), growing very slowly probably due to the compression of the coating oxide layer. The third family is characterized by preferential nucleation and rapid growth around carbide inclusions due to the discontinuity in the oxide at the carbide/oxide interface. The fourth family is found only on the samples having a thick oxide layer, and is characterized by a rapid growth rate, but is not located around inclusions. In this case, the nuclei probably originate at some other oxide discontinuities, such as twins or grain boundaries.

Keywords: Uranium; Hydride formation; Nucleation and growth; Atomic force microscope

1. Introduction

Uranium and uranium alloys react easily with hydrogen to form uranium hydride [1]. The hydriding reaction of massive uranium samples has been reported to start on the surface with (visually observed) hydride nuclei growing on the surface till a full hydride layer is formed [2,3]. The kinetics of the hydrogen–uranium reaction were studied extensively [1,4]. Hot-stage microscope (HSM, see next section) experiments yielded the dependence of nuclei density and growth kinetics on temperature, pressure and also sample microstructure [5].

In the early HSM experiments [2,3], as well as those reported in the present study, more than one family of hydride nuclei was observed. In most cases two families were reported: (a) relatively few nuclei (around 200 mm^{-2}) growing fast till their combined area covers the whole surface, and (b) a much denser family (10^{3}–10^{4} mm^{-2}) of smaller nuclei, growing much slower and sometimes reaching a virtually final size (of 5–10 μm). A typical HSM sequence of pictures describing the development of these two families on pure uranium is presented in Fig. 1. In some cases only one of these families appears and, as will be discussed later on, there are also cases where a third, intermediate growth velocity family was observed.

It was suggested in the early HSM studies [2] that the former (fast growth) family is located at (naturally existing) carbide inclusions. However, this was disputed in a later HSM study [3], where it was claimed that the fast growing nuclei are not correlated with such inclusions.

In the present study, various surface oxide layers were produced by applying different preparation procedures (for both pure and Cr-alloyed uranium), and their effects on the hydride nucleation and growth characteristics were checked. Some of the controversies in the literature may then be accounted for.

A microprobe analyzer (MPA), which includes a scanning electron microscope (SEM) and wavelength dispersive X-ray spectrometer (WDS), was applied

*Corresponding author.

0925-8388/96/$15.00
PII S0925-8388(96)02505-4

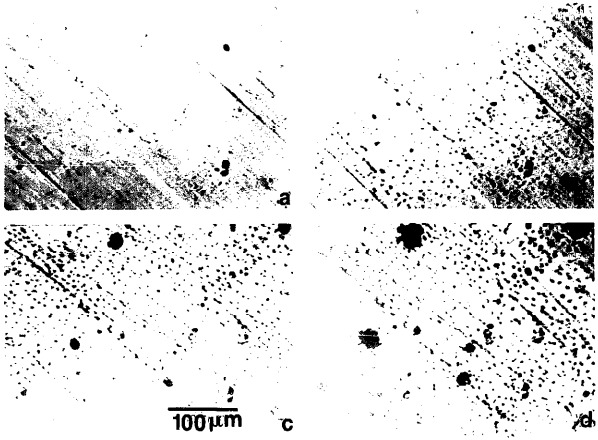

Fig. 1. The sequence (Δt = 30 s between sequential pictures) of the hydrogenation process of pure uranium as recorded by the HSM. Two families of hydride nuclei are clearly observed.

together with the HSM in order to identify the carbide inclusions (Fig. 2, for example) and the hydrogen attack around them, as well as the other types of hydride nuclei. In one case, an atomic force microscope (AFM) was used to observe the submicron structure of a partially hydrogenated sample.

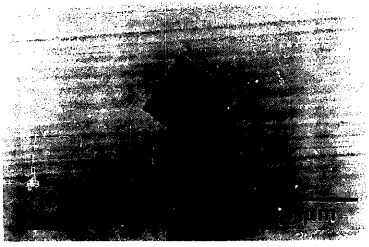

Fig. 2. SEM image of a typical uranium carbide inclusion on a polished surface of pure uranium.

2. Experimental

The HSM assembly consists of a high-vacuum chamber, optically coupled with a microscope. The chamber can be evacuated down to about 10^{-6} mbar and filled with the reaction gas up to a pressure of 1000 mbar. The reacting sample is placed in a specially designed holder incorporating a furnace, capable of heating the sample up to 1100 °C. A thermocouple is attached to the sample, so that a very accurate control of the reaction temperature (±0.1 °C) can be achieved. The microscope is equipped with a video camera and a recorder, so that the process can be monitored continuously. The studies were performed on pure U and on the alloy U–0.1 wt.% Cr. All samples were polished down to 1 μm. All samples were preheated in the HSM at 200 °C for 2 h. The hydrogenation was performed with the samples at temperatures of 50–75 °C. However, variations in the hydriding characteristics, due to temperature variations, are very minor within this range. These temperature variations are, therefore, insignificant regarding the qualitative classification of the nucleation and growth families. The hydrogen pressure for all experiments was 1000 mbar. The transfer of samples to the

MPA was performed in about 15 min, so that no observable changes in the hydride morphological patterns have taken place.

3. Results

3.1. Case study I: pure uranium, thin oxide layer

The sample was polished a short time before introduction to the HSM (without etching), ensuring a thin oxide (a few nanometers, see Section 3.2) formed during the preheating. The two hydride nuclei families, mentioned in the Introduction, were observed (Fig. 3), and the reaction was stopped abruptly at a relatively late stage. The sample was then transported into the MPA apparatus. Fig. 4 presents a SEM image, of about the same magnification as Fig. 3, where the small family can be identified as blisters. An attack around a carbide is also observed. More magnified SEM images are presented in Fig. 5. Fig. 5(a) Fig. 5(b) present a hydrogen attacked carbide inclusion, together with a WDS carbon line scan over it. Also observed are the blisters of the first family. Since the hydrogenation was stopped at a relatively late stage, the blisters are well developed, reaching a size of up to around 10 μm. On top of most blisters one can observe a defect, and concentric cracks are clearly seen on the more developed ones.

A similar pure uranium sample was prepared in the same way, placed into the HSM, and given the same pretreatment. A short hydrogenation exposure was performed and stopped after 1 min, when the first few nuclei of the small family were observed. The sample was then transferred to an AFM apparatus (operated in air) and a scan was performed on a $10\times10\ \mu m^2$ area. A partial $5\times5\ \mu m^2$ scan is presented in Fig. 6. The approximately 1 μm blister-like hydride nucleus is clearly observed, together with many small (submicron) hydride blisters, observed on the scratch lines of mechanical polishing. These features were not observed for a reference sample that had been polished by the same method and not allowed to interact with hydrogen.

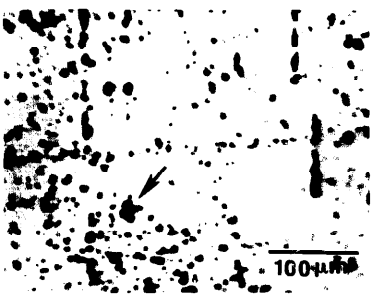

Fig. 3. HSM recording of partial hydrogenation of the Case I sample. A member of the large family of nuclei is marked with an arrow.

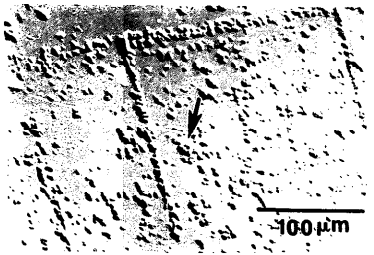

Fig. 4. SEM image of the Case I sample after transformation to the MPA. The hydrogenation around the carbide is marked with an arrow.

3.2. Case study II: U–0.1 wt.% Cr, thin oxide layer

This sample was polished and immediately introduced into the MPA, and a certain area was identified. In particular, a line pattern of four carbide inclusions was identified. A WDS carbon line scan through these inclusions is presented in Fig. 7(a). The sample was then transferred to the HSM, pretreated and partially hydrogenated for a shorter time than in Case I. The hydrogen gas was pumped out, and the sample was transferred back to the MPA. The vicinity of the above indentified carbides was monitored, and its SEM image is presented in Fig. 7(b). Here too the two families of hydride nuclei are clearly observed. The blisters are less developed and no cracks are observed. The defects on top of each blister are, in contrast, well observed. The attack around the carbide inclusions is clear. A more advanced stage of hydride growth around a carbide inclusion is presented in Fig. 8.

Another U–0.1 wt.% Cr sample, prepared identically to the above, was placed in the HSM and given the same preheating procedure. Auger electron spectroscopy used to monitor the Ar^+ sputtering depth profile,

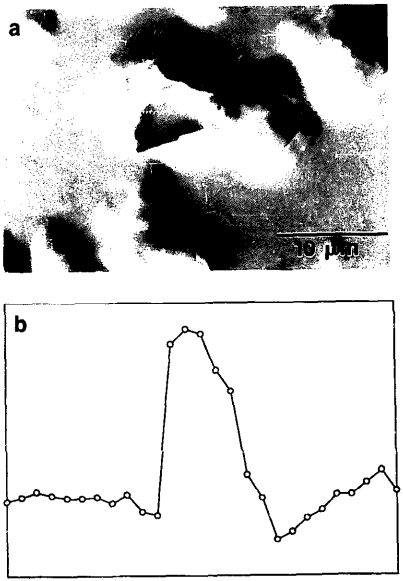

Fig. 5. (a) SEM image presenting the two families of hydride nuclei. The lifting and cracking of the oxide around the attacked carbide is clearly seen. (b) WDS carbon line scan through the carbide inclusion. The scale dimension of (a) and (b) is identical.

Fig. 6. AFM scan of a pure uranium sample after a short hydrogenation.

performed on the sample, yielded an average oxide path depth of about 4 nm.

3.3. Case study III: pure uranium, thicker oxide layer

This sample, after polishing to 1 µm, was stored under a vacuum of about 1 mbar for a couple of weeks. During this period the sample acquired a less shiny, brownish appearance, indicating a thicker surface oxide layer than that of the two previous samples. Following the standard preheating in the HSM, a partial hydrogenation was performed.

Two families, both with a low hydride nuclei density (ca. 200 mm^{-2}) were observed: one with a moderate growth rate, around 0.9 µm min^{-1} (compared with the family of large nuclei of the former two cases, around 5 µm min^{-1} for Case I and 3 µm min^{-1} for Case II); the other having a faster growth rate, comparable with that of the former cases, around 6 µm min^{-1}. The family with small numerous nuclei was not observed in

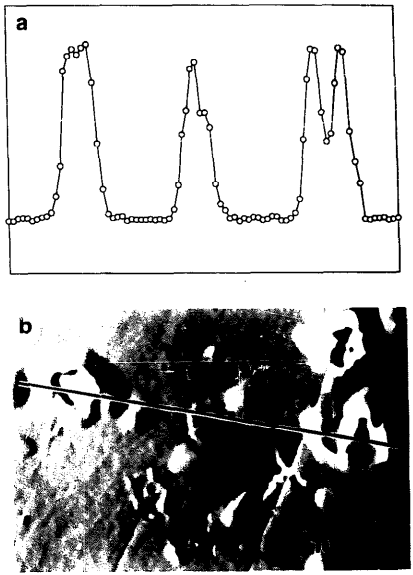

Fig. 7. (a) Case II: WDS carbon scan through the line of carbide inclusions on the surface of U–0.1 wt.% Cr prior to hydrogenation. (b) SEM image of the above carbides and their vicinity after partial hydrogenation. The scale dimension of (a) and (b) is identical.

this case. However, when the sample was transferred to the SEM apparatus, the family of small hydride blisters was observed (Fig. 9). The very small size, around 1 μm, of the blisters is the reason why this family was not observed by the HSM. The medium rate family was identified as carbide centered (Fig. 10).

Fig. 8. SEM image of a more advanced hydrogen attack around a carbide.

Fig. 9. SEM image of a blister-like hydride nucleus on the surface of the Case III sample.

The faster growing family does not seem to be located around any identified specific location.

3.4. Case study IV: U–0.1 wt.% Cr, thicker oxide layer

This sample was mechanically polished down to 1 μm and then electrolytically polished and etched. This produces a thicker oxide layer of around 50 nm [6]. The sample was placed in the HSM and the carbide inclusions could be clearly seen as a result of this pretreatment. Following the standard preheating, a partial hydrogenation was performed. Only one family of a few hydride nuclei was observed, growing at a moderate rate, around 0.8 μm min^{-1}. The origin of this family was not around the carbide inclusions, and no specific location could be identified. The sample was transferred to the SEM and two additional families of hydride nuclei, not observed in the HSM, were detected. The first is the family of many small (around 1 μm) blisters, also observed in Case III (Fig. 9). The carbide inclusions that seemed to be unattacked in the HSM appeared to be attacked in an unusual way, which looks like swelling around the carbide (Fig. 11).

4. Discussion

In the present study, four cases, two of pure uranium and two of U–0.1 wt.% Cr, were chosen. The heat pretreatment, reaction pressure and temperatures were similar for all cases. The only significant parame-

Fig. 10. SEM image of a carbide site hydride nucleus on the surface of the Case III sample.

Fig. 11. SEM image of hydrogen attack around a carbide inclusion on the surface of the Case IV sample.

ter, varied between experiments, was the preparation of the sample, causing different oxide layers.

The SEM and AFM images clearly show that the different families of hydride nuclei relate to different surface sites. The discussion will, therefore, be separate for each family, starting from the most dense and smallest size of nuclei, and then going up in size.

4.1. First family: submicron, very dense blister-like nuclei on mechanical polishing scratches

AFM measurements were performed only on the Case I sample, where the above family was observed (Fig. 6). The sharp features of the polishing scratches are likely to induce irregularities in the oxide formed on top of them. These irregularities are probably the channels for preferential hydrogen flow and hydride phase nucleation, as indicated by the appearance of submicron blisters on the scratches as observed with the AFM. These submicron features were not observable using the other techniques employed in the present study. Since the size of these nuclei is within the submicron range, they seem also to grow under the oxide compression without cracking it.

4.2. Second family: blister-like, small nuclei, with a high nucleation density and low growth rate

Fig. 5(b) (Case I), Fig. 7(b) (Case II) and Fig. 9 (Case III) show clearly that the small blister-like hydrides develop under the oxide layer, without cracking it, at least at the stage where the hydrogenation was stopped (in Case I, concentric cracks can be observed on the more developed blisters). A defect can be observed on each blister, probably being the channel of preferential hydrogen flow through the oxide to the metal interface. The ordered, non-random structure of some of the nuclei on the surface of the Case I sample may suggest non-random defects, located mostly on scratches. The slow growth rate of this family, in comparison with the other families, is probably caused by the compression exerted by the oxide layer on top of the hydride which develops underneath. The blisters reach a relatively large (5–10 μm) size for Cases I and II, where the oxide thickness is about 4 nm. For Cases III and IV, where a significantly thicker oxide layer exists, the blisters, experiencing a higher compression during swelling, reach a much smaller size (around 1 μm).

4.3. Third family: nucleation around carbide inclusions

Before embarking on the analysis of the nucleation and growth of hydride around carbide inclusions, a distinction should be made between the pure uranium and the U–0.1 wt.% Cr samples. The amount and size distribution of the carbide inclusions in pure uranium (around 80 wppm C) and U–0.1 wt.% Cr (around 500 wppm C) was found to be significantly different. While on the surface of pure uranium about 200, almost unisize (approximately 7 μm diameter) inclusions per square millimeter were detected, for U–0.1 wt.% Cr the number is about 2000 mm^{-2}, with a broader size distribution (between about 2 and 7 μm). In spite of this difference, the number of fast growing, large-size families of hydride nuclei was about 200 mm^{-2} in both cases. A detailed analysis of the correlation between the size of the carbide and the hydrogen attack around it indicates that mostly relatively large (greater than 3 μm) inclusions are attacked. Hence, the larger number of smaller inclusions present on the U–0.1 wt.% Cr samples were not contributing to the family of fast growing hydride nuclei.

A possible explanation is as follows. Since the carbide is a physically held inclusion, having a lower thermal expansion coefficient ($13\times10^{-6}\,°C^{-1}$ [7]) than that of the uranium matrix ($44\times10^{-6}\,°C^{-1}$ [8]), a gap is formed at the carbide/uranium interface when heating the sample (during preheating treatment in the HSM). The uranium surface in this gap is oxidized (as well as the whole surface) by the residual gases in the HSM (base pressure about 10^{-6} mbar). Cooling the sample induces pressure on the oxide at the carbide/uranium interface. These dimensional changes (and hence also the pressure when the carbide/oxide/uranium zone is cooled) is proportional to the dimensions of the carbide inclusion. Up to a certain size the oxide may withstand this pressure. Above this limiting size (in this case about 3 μm carbide) the oxide is cracked under the thermal compression, hence creating a discontinuity that enables an easy flow of hydrogen inwards (preferential hydrogenation) and an easier expansion path of the formed hydride which easily breaks that cracked oxide (unlike the case of the family of small nuclei). This process can clearly be seen in Figs. 5,7 and 8,10, which acounts for the higher rate of hydride growth observed in this family.

A different behavior is observed for Case IV (Fig. 11). The swelling under the oxide indicates a preferential hydride formation at the uranium/carbide interface, probably due to a relatively easy entry path of hydrogen through the oxide/carbide discontinuity. However, the oxide, formed mostly by the electrolytic polishing and etching, is thick and strong enough to withstand the pressure applied by the expanding hydride without breaking. At a later stage, the hydride formation is stopped as the pressure applied by the oxide is high enough.

It should be pointed out that even though the size effect of the carbide inclusions has been accounted for

by the above discussion, there is still an unclear point in that approach. Although all fast growing hydride nuclei of the thin oxide cases (i.e. I and II) are located at larger size carbide inclusions (not below 3 μm), not all inclusions within this size range are attacked by hydrogen in the same way. An example of what looks like an approximately 3 μm unattacked inclusion can be seen in Fig. 7(b). A higher magnification shows an initial hydrogenation at some sections of the carbide/uranium interface. Hence, there is presently no explanation as to why some carbides of a certain size are attacked and others, having the same size, are not, or why the attack on them is delayed. This is probably related to the specific nature of the carbide/metal interface, that is different for different carbides. More experiments with an effort to examine submicron features of interfaces and defects (by the AFM for example) may enable a better understanding of this behavior.

An additional possible contribution to preferential hydrogenation at the uranium/carbide interface is stress induced (preferential) hydrogenation. This effect had already been observed in macroscopic systems [9,10]. The uranium matrix around the carbide inclusion is strained since, during cooling from the melt (in the casting process), the uranium matrix contracts around the inclusion due to its higher thermal expansion coefficient, thus inducing stress around the interface. Preferential oxidation due to this stress had been observed [11], and it is reasonable that a similar effect with hydrogen should occur.

4.4. Fourth family: fast growing nuclei around other defects

The HSM experiments performed on the thicker oxide case studies (III and IV) revealed a family of relatively few hydride nuclei, growing at a speed similar to that of the 'carbide family' of the thin oxide cases (I and II) but not located near any identified inclusion (in fact, the development of the hydride around carbide inclusions in these cases is slower, as described before).

It thus seems that when a thin layer (a few nanometers) of oxide is present, it is adherent and continuous (except for the discontinuities around inclusions). The mismatch between metal and oxide unit cells, the discontinuities in the metal microstructure (such as twins, grain boundaries, etc.) and also sharp features like polishing scratches probably cause strain and also defects, but not macroscopic cracks and discontinuities (Fig. 6, the AFM scan proves that scratches are defective but the size of the hydride nuclei is too small to originate from macroscopic gaps in the oxide).

For thicker oxides, however, the oxide probably starts to crack and discontinuities are formed on it. It has recently been shown [5] that for thicker oxides there is a correlation between the location of oxide cracking and the microstructural characteristics of the metal beneath. These gaps are, in these cases, the most preferential paths for hydrogen to the metal and also weak lines, enabling the lifting and breaking of the oxide, thus being the sites of the fastest growing family of nuclei.

5. Summary and conclusions

Four case studies of hydride nucleation and growth on the surfaces of pure uranium and U–0.1 wt.% Cr with thin and thicker oxide layers were studied. It has been established that the different types of defect in the oxide result in different classes (or families) of hydride nuclei, characterized by different nucleation densities and growth rates. The classification of families, going from the smallest to the largest, is as follows.

(i) *The submicron family: very dense nucleation along mechanical polishing scratches.* This family was observed only in the AFM scan (Fig. 6), performed on a sample of the Case I type, but is assumed to exist on all samples polished mechanically. The sharp features of the scratches probably induce a defect in the oxide growth that enables a slight preferential hydride flow to the metal and dense nucleation along the polishing lines. This nucleation is in the shape of submicron blisters. The hydrogen flow and oxide strength are such that this family is kept to a small size that is not observable by the HSM and SEM.

(ii) *Blister-like nuclei growing under the oxide.* This family, observed for all four cases, consists of nuclei developing under the oxide by the preferential hydrogen flow through some defects, (unidentified but having about a constant density of around 2000 mm^{-2}) observed on the top of the blisters. The final size of blisters is dependent on the thickness of the oxide. For relatively thick oxides the typical size is approximately 1 μm. For thin (around 5 nm) oxides, it can reach a size of about 10 μm. The swelling is under the (intact) oxide, and the pressure exerted by it slows down the growth rate of the nuclei. Concentric cracks can be observed on the more developed blisters under a thin oxide (Fig. 5(c)).

(iii) *Fast growing nuclei around carbides.* This family, observed in the thin oxide cases, wes clearly identified in SEM images. The discontinuity in the oxide, inherent to the carbide/uranium interface, is strongly affected by the thermal pretreatment, which cracks the oxide around that interface. The extent of this effect is supposed to be dependent on the size of the carbide inclusion. There is, indeed, a correlation, for U–0.1 wt.% Cr, between the size of the carbide

and the hydrogen attack around it (mostly above 3 μm size carbides are attacked). However, in this case not all of the above 3 μm carbides are attacked (only about 10% of them). For pure uranium, however, all the carbides are large, and the density of carbides is comparable with that of the fast growing nuclei family. The discontinuity in the oxide also enables its lifting and breaking by the hydride (clearly observed in the SEM images), causing the fast growth rate of this family. There may be some contribution to the hydrogenation from the stress around the carbide and from a galvanic effect between the carbide and the uranium matrix. The relative size of these possible contributions is unknown.

(iv) *Fast growing nuclei around other defects.* This family is observed for the thicker oxide samples. When a thick oxide is formed, discontinuities in the surface microstructure (such as twins, habit planes and grain bounderies), and sharp geometrical features, may lead to discontinuities in the oxide layer. These discontinuities provide an easy path for hydrogen ingress and a mechanically weak location, enabling the cracking of the oxide by the expanding hydride. It seems that, for the thicker oxide cases, the role of the carbide inclusions in providing a preferred growth location for the hydride is less dominant than the role of these discontinuities.

As stated in the Introduction, these four families seem to give a consistent view of the site-related nucleation and growth of hydrides on uranium surfaces within the applied experimental conditions (i.e. pressure and temperature). Changing the pressure and temperature causes complex effects (e.g. selective appearances of only part of these families), and more experimental effort is needed in order to evaluate and understand these effects.

Acknowledgments

The authors wish to acknowledge the technical support of Mr. Mimon Cohen and Mr. Alexander Adler. The AFM observations were made by Dr. Eithan Grossman from the Soreq Nuclear Research Center. This study was supported by a grant from the Israel Atomic Energy Commission and the Israel Council for Higher Education.

References

[1] M.H. Mintz and J. Bloch, *Progr. Solid State Chem., 16* (1985) 163.
[2] L.W. Owen and R.A. Scudamore, *Corrosion Sci., 6* (1966) 461.
[3] J. Bloch, F. Sinca, M. Kroupp, A. Stern, D. Shmariahu, M.H. Mintz and Z. Tadari, *J. Less-Common Met., 103* (1984) 163.
[4] J. Bloch and M.H. Mintz, *J. Less-Common Met., 81* (1981) 301 and references cited therein.
[5] D. Moreno, R. Arkush, S. Zalkind and N. Shamir, *J. Nucl. Mater.*, in press.
[6] E. Swissa, N. Shamir, M.H. Mintz and J. Bloch, *J. Nucl. Mater., 173* (1990) 87.
[7] W.D. Wilkinson, *Uranium Metallurgy*, Vol. 2, Interscience, New York, 1962, p. 953.
[8] J.J. Katz and E. Rabinowitch, *The Chemistry of Uranium*, Dover Publications, New York, NY, 1951, p. 137.
[9] S. Zalkind, R. Ashkenazy, S. Harush, D. Halperin, D. Moreno, E. Abramov and A. Venkert, *J. Nucl. Mater., 209* (1994) 169.
[10] P.K. De, I.T. John, V.V. Raman and S. Banerjee, *J. Nucl. Mater., 203* (1993) 94.
[11] A. Venkert, M. Aizenshtein, R. Arkush and N. Shamir, submitted to *J. Nucl. Mater.*